

## Mineralogy and Geochemistry of Hydrothermal Alterations in Shoja Abad Region along Great Qom – Zefreh Fault in Northeast Esfahan



Mozhgan Poormansouri<sup>1</sup>, Mohammad Hossein Razavi<sup>1\*</sup>, Afshin Ashja Ardalan<sup>1</sup>,  
Mohammad Ali Makkizadeh<sup>2</sup>, Mohammad Khalaj<sup>3</sup>

<sup>1</sup>Geology Department, Tehran North Branch, Islamic Azad University, Tehran, Iran

<sup>2</sup>Geology Department, University of Esfahan, Esfahan, Iran

<sup>3</sup>Geology Department, Payam-e Noor University of Tehran, Tehran, Iran

Corresponding author: \* razavi.khu@gmail.com

Received: July 27, 2018; Revised: September 15, 2018; Accepted: September 25, 2018

**Abstract :** Compared to other alterations, Rare Earth Elements (REEs) do not indicate remarkable mobility in Shoja Abad Region. Low mobility of REEs and increase in heavy rare earth elements (HREEs) in the propylitic zone are associated with high pH level and low water-content of the rocks in the respective region and transfer of the respective elements to the clay minerals of the kaoline family (halloysite and kaolinite). In the region under study, depletion alteration of all REEs is observed with slight differentiation from the HREEs. This is reflective of formation of this alteration zone in an environment with high pH and temperature. Evidently, the respective conditions lead to leaching of all rare earth elements. In the vicinity of Qom-Zefreh faulting zone in the region under study, alterations can be observed resulting from geothermal solutions of rising calc-alkaline andesite magma. The most significant attribute of the respective section is presence of enclaves of oceanic crust composition (~Upper Cretaceous) and uplifting of the dark-colored masses during rise of calc-alkaline magma.

**Keywords:** Hydrothermal alteration, Shoja Abad, Uremia–Dokhtar Belt, Qom – Zefreh Fault

### 1- Introduction

Shoja Abad Region is located between 33° 07'N and 33°26'N latitudes and 51°27'E and 51°56'E longitudes in the Central Iran magmatic belt (Agha Nabati, 2006), 120 km to the northeast of Esfahan (Fig. 1). The area is located in the southwestern side of Ardestan geological quadrangle (Agha Nabati, 2006), hosting mineralization, leucocratic and pyroclastic rocks, and Eocene lavas with acidic composition and porphyry – breccia texture. The Eocene igneous group has been invaded by Neogene–Paleo- Pleistocene magmatism phase, outcropping in the northwest of the region with the composition of basalt, pyroxene andesite, and trachyandesite.

The Central Iran Zone, especially Urmia–Dokhtar Magmatic Belt (UDMB) hosts extensive magmatism in the Cenozoic times. During geological time, the respective igneous rocks have undergone thermal alteration (Mehvari 2009, Namnabat 2011, Khodami 1998, Taghipour and Mor, 2008). Alunite and jarosite are often formed due to oxidation of sulfide minerals as gossan in the zone of oxidation. The study aims to identify minerals and determine the mechanism of formations of the respective minerals in volcanic

rocks in the area to help in prospecting and exploration of metallic veins, particularly epithermal gold deposits.

### 2 – Research Methodology

A sampling program was carried out to collect samples, field-photographs along with demarcation of contacts using GPS. Petrological and petrographical studies were made to determine the mineralogical, petrological compositions, micro-textures and their mutual relationships were determined. ICP-MS and SDF techniques were used to measure the contents of principal elements, rare elements, and REEs of the analyzed samples.

### 3 – Discussion

As mentioned above, the Eocene igneous group has been invaded by Neogene–Paleo- Pleistocene magmatism phase, outcropping in the northwest of the region with the composition of basalt, pyroxene andesite, and trachyandesite. The same magmatism has probably resulted in occurrence of different alterations such as silicification, sericitization, chloritization, and kaolinitization in the regional rocks.

The mineral index of alunite-natrualunite-jarosite were observed in the stock-, box work, veinlets, nodules, coatings, and crusts in diverse colors (fawn to brown, orange, creamy and milky-white (Parsapour, 2004) in association of barite, pyrite, hematite, microcrystalline quartz and cryptocrystalline quartz, turquoise, malachite, and azurite (Taghipour, 2007). Pterography shows that alkali feldspar, chlorite, and sericite as the principal constituent minerals (Figs. 2, 3, 4, and 5). Alkali feldspar have been generally altered into extremely tiny kaolinite clay mineral, chlorite, and quartz. Alunite-jarosite are detected in honey yellow colour under PPL and high interference colors between cross Nocolsas substitution, and/or scattered into phenocrysts of altered alkali feldspars and/or as a coating over them. The respective mineral is also seen independently in complex of quartz crystals and intra-mineral texture. In certain cases, minute pseudo-cubic and lozenge-shaped crystals are observed in a matrix of iron oxides.



Fig. 2 – Outcrops of rocks in the area under study



Fig. 1 – The area under study

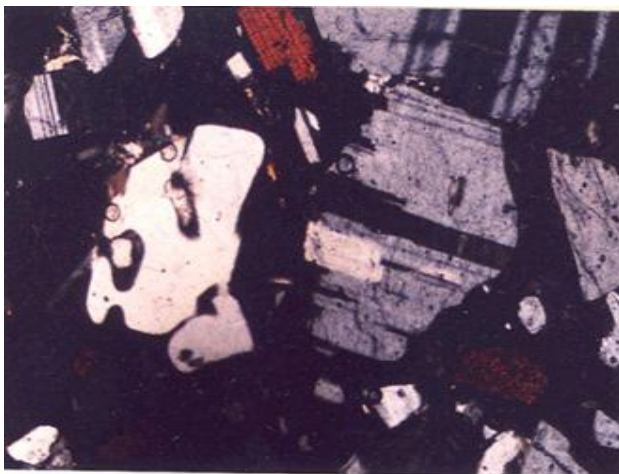


Fig. 3 – Porphyry texture in volcanic rock before quartz alteration with resorbed margins along with plagioclase phenocrysts XPL×100

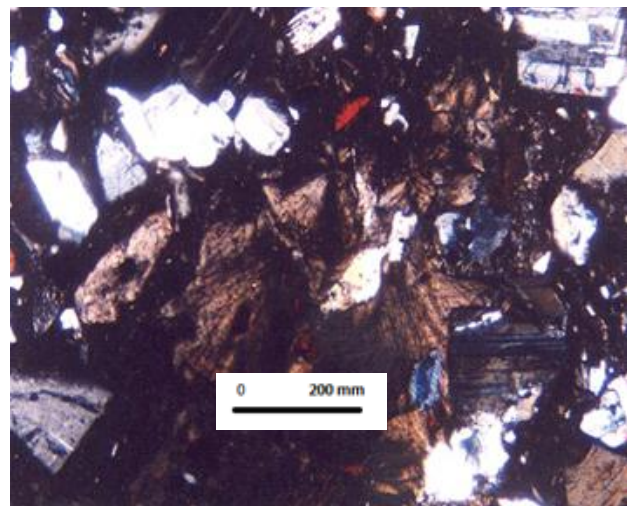


Fig. 4- Matrix alteration and spherulites XPL×100

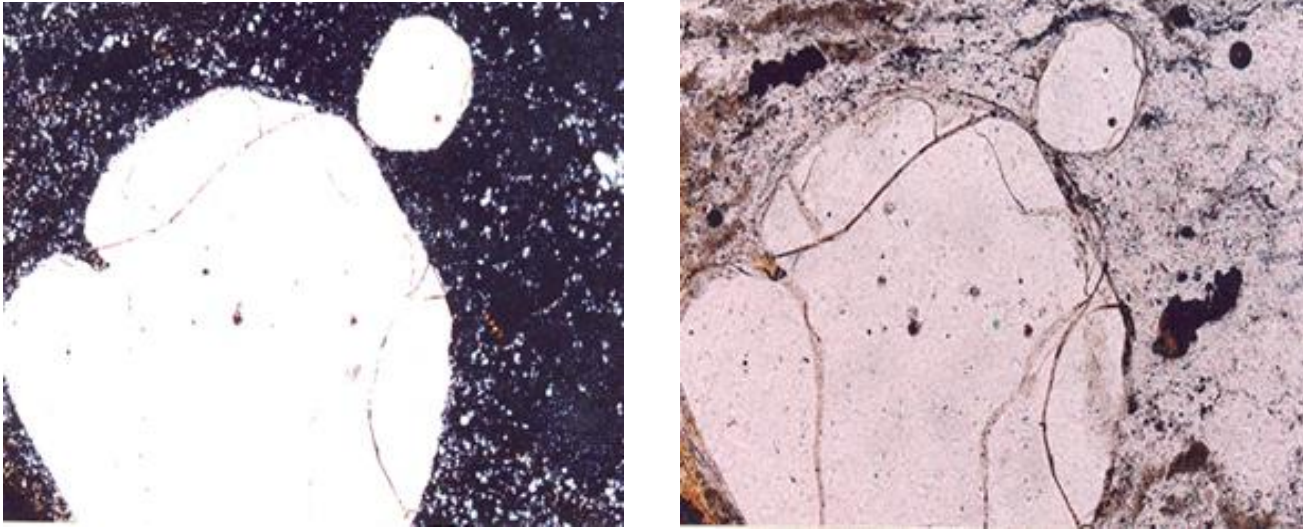


Fig. 5–Quartz in phenocryst form with rounded margins and embayed resorption in a matrix of glass and crystal PPL and XPL×100

#### 4 – Altered Minerals in the Area of Study

##### 4.1 – Jarosite

Jarosite family minerals (Fig. 6 occur secondary phases showing oxidation of sulfide ores together with acidic rocks (Nordstrom, 1977; Alpers and Brimhall, 1989; Dutrizac and Laniboi, 2000; Stoffregen *et al.*, 2000). Minerals of Jurassic family (when  $B = B = Fe^{3+} > Al^{3+}$ ) are a subgroup of alunites family  $[AB_3(XO_4)_2(OH)_6]$ . In the respective formula, “A” equals  $NH_4^+, H_3O^+, Rb^+, Ag^+, K^+$ , and Na, “B” represents  $Al^{3+}, Cr^{3+}$ , and X, and  $Fe^{3+}$  equals P-As<S (Jambor, 1999, Dutrizac & Jambor, 2000). The following equations have been proposed for jarosite occurrence.

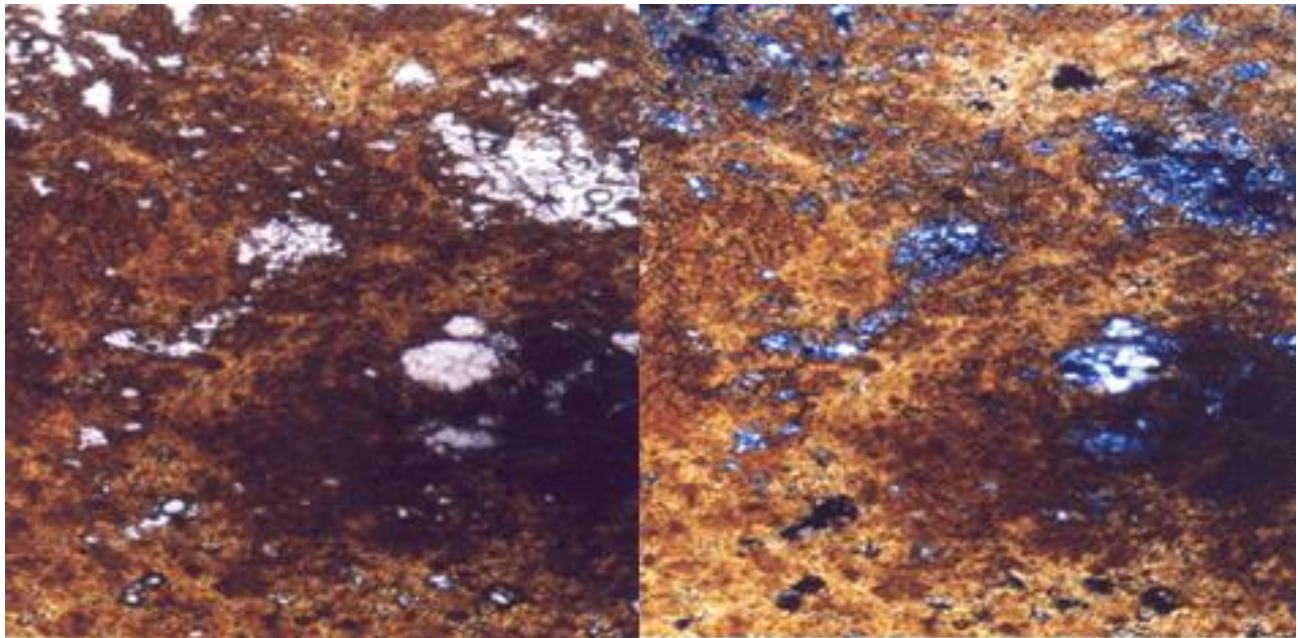
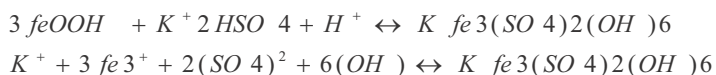


Fig. 6 – Accumulation of tiny and compact crystals of jarosite in a quartz matrix



Direct conversion of sericite into jarosite is possible via the following equation (TAQIPOUR & MOR, 2008)



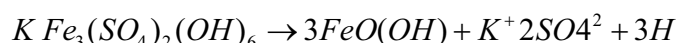
The following reaction occurs at 400 °C (Desborough *et al.*, 2010)



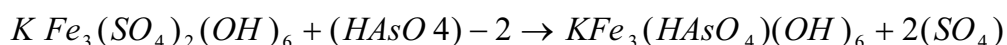
Jarosites are formed in two forms (Lewis *et al.*, 1997):

- 1 – Jarosites of primary hydrothermal type
- 2 – Jarosites enriched as a result of weathering

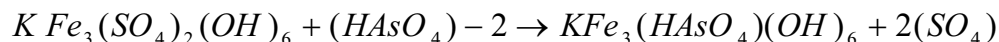
The first type jarosites were deposited in the delayed hydrothermal stage along with barite and fluorite such that acidic geothermal waters are mixed with the oxidized underground water and jarosite will ultimately form at a temperature ranging from 80 to 200 °C. The second type jarosites occurring are commonly referred to as supergene jarosites formed due to weathering and oxidation of pyrite. The hydrothermal jarosites are normally formed in epithermal environments under high oxidation conditions, near the ground surface, and with low pH and show better crystalline structure at higher temperatures (100 to 300 °C) as compared to supergene jarosites (Desborough *et al.*, 2010). Jarosites precipitate from waters rich in sulfate in pH range from 1 to 3 (Alpers *et al.*, 1989). Jarosite can be used in studies of evaluation from two directions for determining points with high acidity (Swayze *et al.*, 2000) and can generate acid through the following reaction (Desborough *et al.*, 2010).



Stability interval of jarosites is from pH value of 0.5 to 5. All natural jarosite samples are a solid solution with the general formula  $\text{KFe}_3(\text{SO}_4)_2(\text{OH})_6$ ; natrojarosite with the formula and hydroniumjarosite with the formula  $(\text{H}_3\text{O})\text{Fe}_3(\text{SO}_4)_2(\text{OH})_6$ .



As per results of the analysis of jarosite in the region (Table 1), the respective diagram cannot be used for classification of the jarosites in the region due to presence of aluminum in the its composition because some amount of Al has replaced Fe. Hydronium jarosite is formed under conditions of intense sulfide oxidation and/or where Na and K elements are limited (Dutrizac and Jambor, 2000). Hydronium-bearing jarosite instances are observed in relatively younger supergene samples and are instable at geological time scale (Desborough *et al.*, 2010). The experiments indicated that  $\text{AsO}_4$  are strongly absorbed by it at pH value of 2 (Wise, 2000).  $\text{AsO}_4$  is combined with Fe oxides and hydroxides and substitute octahedral layers of it in (001) crystallographic plane (Bissig *et al.*, 2002). Potassium enters jarosite structure at approximate pH value of 1.6. In certain cases,  $\text{AsO}_4$  substitution by  $\text{SO}_4$  is observed in sulfide minerals based on the following equation (Dutrizac and Jambor, 2000)



Due to similarity of ionic radius of Ca and Pb with K, the mentioned cations are able to substitute K.

In supergene environment, jarosite is stable in pH range of 2 to 4 whereas stability conditions of alunite happen in pH range of 3 to 6.

### 5 – Geochemistry of REEs in the Regional Alterations

In order to analyze behavior of the respective elements, frequency pattern of REEs is plotted in the altered rocks of different zones and less altered rock (equivalent to fresh rock in the region). REE pattern in less altered rocks can be clearly reflective of the initial composition of the unaltered parent rock (Rollinson, 1993). Here, behaviors of rare earth elements in different alteration zones of Shoja Abad are analyzed in comparison with host volcanic rock (less altered rock). Analyses of 5 samples have been used for this purpose (Table 1)

Table 1 – Behavior of rare earth elements in different alteration zones of Shoja Abad

Sample	La	Ce	Pr	Nd	Sm	Eu	Gd	Tb	Dy	Ho	Er	Tm	Yb	Lu
Lessaltered	41.61	72.87	7.99	28.77	4.81	1.44	3.49	2.48	0.48	0.44	1.1	0.15	0.89	0.14
Phyl	42.9	71.7	7.67	26.21	3.7	0.86	1.8	0.19	0.8	0.14	0.45	0.08	0.62	0.12
Proy	27.8	48.23	5.20	19.05	3.39	0.99	2.64	0.39	2.16	0.42	1.1	0.16	1.02	0.16
Argil	23.15	42.94	4.87	18.38	3.47	1.04	3.52	0.69	5.3	1.19	3.35	0.46	2.72	0.88
Silicic	13.76	22.11	3.21	7.2	1.13	0.2	0.7	0.31	0.94	0.22	0.49	0.06	0.45	0.06

### 5-1 – Propylitic Zone

An overview of the chondrite-normalized REE pattern (Fig. 7) reveals that HREEs exhibit depletion compared to LREEs, which might have resulted from epidote deficiency in the samples of this zone because epidote is capable of absorbing HREEs. Based on chondrite-normalized diagrams of rare earth elements, a magmatic series can be distinguished such that the diagram shows a declining trend for the alkaline, calc-alkaline and shoshonite magmas and flat or slightly ascending trend for the magmas of tholeiitic series. Based on this evidence and taking into account other data, the samples belong to calc-alkaline magma series (It shall be noted that propylitized samples exhibit lowest geochemical mobility among rare elements. Thus, they can be used for petrogenesis). One of the signs of subduction is high ratio of LREE/HREE (Zanetti *et al.*, 1999). One of the attributes of propylitic facies is LREE depletion in samples of the respective zone compared to the original rock. This depletion is due to release of these elements as a result of decomposition of primary silicate phases of the rock such as plagioclase, amphibole, and biotite by means of CO<sub>2</sub>-bearing solutions (Wenlandt and Harrison, 1979). Compared to other alterations, REE content does not indicate remarkable mobility in this zone. Generally, low mobility of rare earth elements in propylitic zone can be attributed to high pH value and low ratio of water to rock.

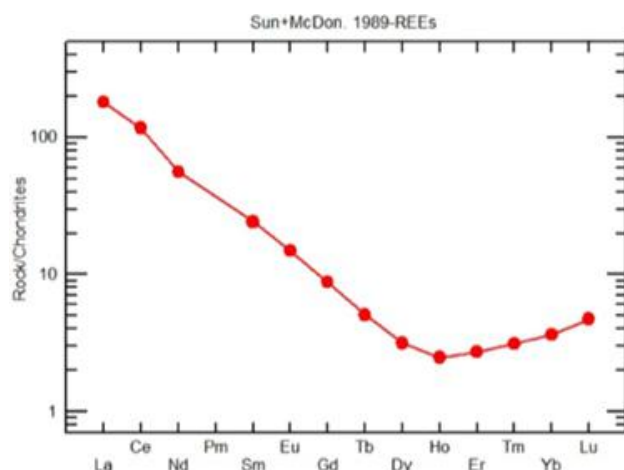


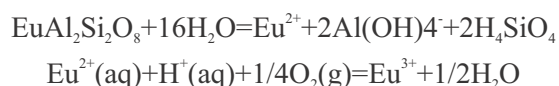
Figure 7 – Chondrite-normalized pattern in propylitic zone

### 5-2 – Phyllic Zone

This alteration, also known as quartz-sericite alteration, occurs as a result of reduction in  $ak^+/aH^+$  or reduction in the temperature of the hydrothermal fluid (as compared to potassic alteration). REE enrichment in phyllic zone can be attributed to partial instability of REE-bearing complexes which lead to deposition of REEs in this zone due to reduction in concentration of dissolved complex ions and/or relative increase in pH. Phyllosilicates and goenites might cause enrichment of rare earth elements via adsorption as the experimental studies (Laufer *et al.*, 1984) and (Aja, 1998) on kaolinite corroborated the fact that the secondary minerals are capable of controlling behavior of rare earth elements (Fulignati *et al.*, 1998).

Overall, negative Eu anomaly is among the pattern characteristics of phyllic zone, as controlled by the fluid pH, sericitization of feldspars, fluid temperature and oxygen fugacity (Bau, 1992). REE depletion in this zone results from complete destruction of feldspars.

Theoretically, Eu is present in the structure of plagioclases and is released as  $Eu^{2+}$  in hydrothermal solutions and is oxidized under oxidation conditions at low temperature and pressure through the following equation into a 3-capacity state:



Alderton *et al.* (1980) studied Eu behavior during supergene alteration and demonstrated that Eu decreases during sericitization of plagioclases and alkali-feldspars. They proposed that the  $Eu^{2+}$  released from feldspars in

hydrothermal solutions cannot enter sericite or illite structure owing to similar ion radius with Sr and Ca. As a result, it is transported and causes negative Eu<sup>2+</sup> anomaly. Magnitude of the respective anomaly is mainly controlled by the ambient pH.

The results acquired from studies are indicative of remarkable difference in behavior of REEs in the alteration zone of the region under study. Pattern of REEs was almost similar to that of the less altered rock and exhibits a general trend of depletion in REEs.

In the phyllic facies, pattern of REEs overlaps and is the same as the one in unaltered equivalent rock. However, depletion of the respective samples is clearly noticeable in HREEs (Fig. 8).

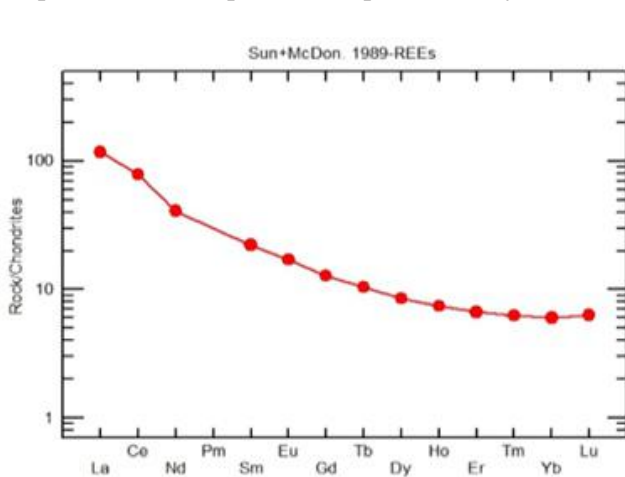


Fig. 8 – Chondrite-normalized pattern in phyllic zone

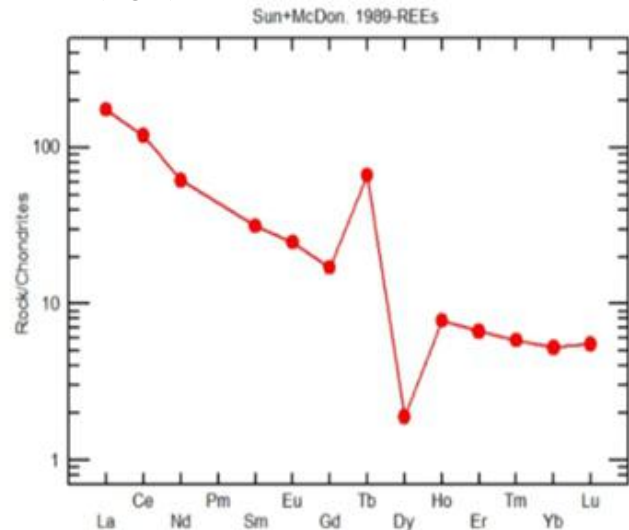


Figure 9 – Chondrite-normalized pattern in argillic zone

### 5-3-Argillic Zone

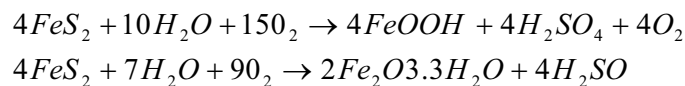
Heavy rare earth elements (HREEs) in the argillic facies show the largest amount compared to other altered samples as well as the original rock. Chondrite-normalized argillic samples (Fig. 9) demonstrate a relatively flat pattern in HREEs and they are more abundant in HREEs compared to intact rock. Increased HREEs in this zone compared to intact rock indicates an increase in pH of the environment and transformation of the respective elements into clay minerals of kaoline family (halloysite and kaolinite) (Lufaur *et al.*, 1984).

#### 5-3-1-Alunite

Alunite is present as a typical mineral in advanced argillic alteration zone (Figs. 10, 11, 12, 13, 14, and 15) and epithermal systems of high-sulfur (HS) type (Scott, 2000). Presence of alunite and jarosite are suggestive of the fact that acidic volcanic rocks have been altered in an environment with exceeded activity of H<sup>+</sup> and SO<sub>4</sub><sup>2-</sup>. H<sub>2</sub>S might produce HSO<sub>4</sub> as a result of oxidation and/or magmatic SO<sub>2</sub> can produce H<sub>2</sub>SO<sub>4</sub> via reaction with water.



High acidity of the environment can be attributed to oxidation of sulfides under alteration conditions



The above mentioned reactions cause increase in acidity of the environment and alteration of aluminosilicates for alunite formation.

Alunites originated from hypogenesis of fluids containing large amount of magmatic vapors are formed in magmatic hydrothermal systems, active volcanoes and HS-type epithermal ores in the alteration zones. In the respective environments, gaseous vapors rich in HCl, SO<sub>2</sub>, HF, and H<sub>2</sub>S are released from magma during cooling. The magmatic gases are mixed with underground waters when they reach the shallow parts. Consequently, they will have a temperature ranging from 250 to 300 and acidic pH value (Hedenquist & Eribas, 1989)

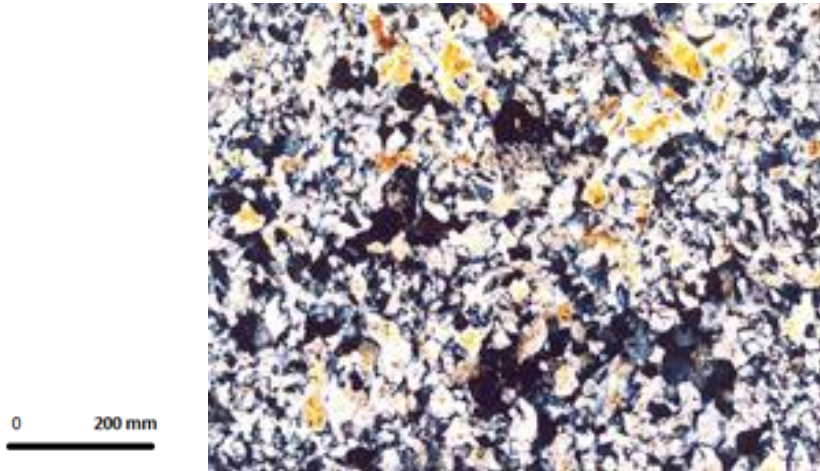


Fig. 10 - Tiny quartz crystals together with alunite XPL×100

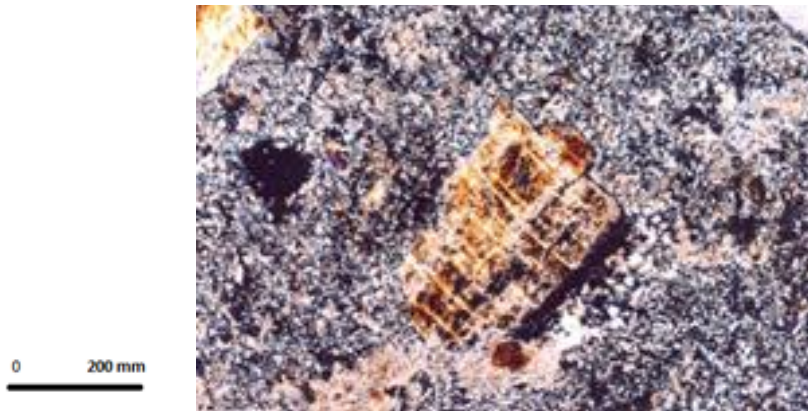


Fig. 11 – Feldspar phenocryst as residue of porphyry texture of volcanic rock in a fine-grain matrix of quartz and alunite XPL×100



Fig. 12 – Argillic, advanced argillic, and propylitic alteration zones



Fig. 13 – Alteration zones along the great northern – southern Zefreh – Qom Fault



Fig. 14 – View of argillic alteration zone and propylitic, siliceous, and advanced argillic alteration can be seen in the background as protruding and scattered siliceous masses



Fig. 15 – Jarosite and gypsum crystals growing on the fracture surface of the altered host rock

#### 5–4–Silicic Zone

Based on the conducted zones (Wood, 1990), the conditions governing the siliceous zone include temperatures below 300 °C, low pH, high oxidation and sulfur abundance. The significant factor of the complex in this zone is sulfate ion. Severe decline of rare earth elements (REEs) is observed in the respective zone, which is associated with acidity of fluids and decomposition of primary minerals under very low PH conditions (PH<2) (Fulginiti and Sbrana, 1998; Bau, 1992). Identical potential of LREEs and HREEs in formation of stable sulfate complexes are among the similar behavior contributors of the aforementioned elements during the respective alteration (Wood, 1990; Haas *et al.*, 1995). In these alteration, there is a depletion of all REE with a small separation of HREE (Figs. 16, 17). This state is suggestive of formation of the respective alteration zone in an environment with low temperature and pH. Obviously, such conditions lead to leaching of entire rare earth elements.

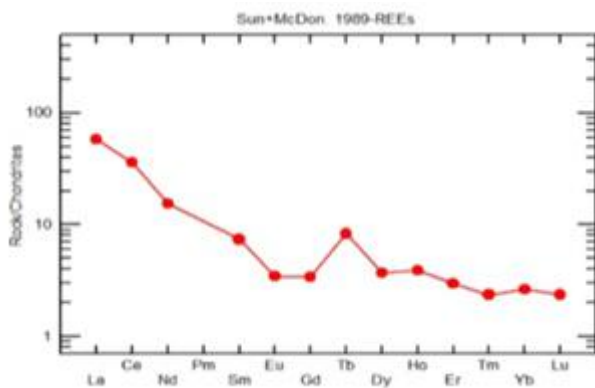


Fig. 16 – Chondrite-normalized pattern in silicic zone

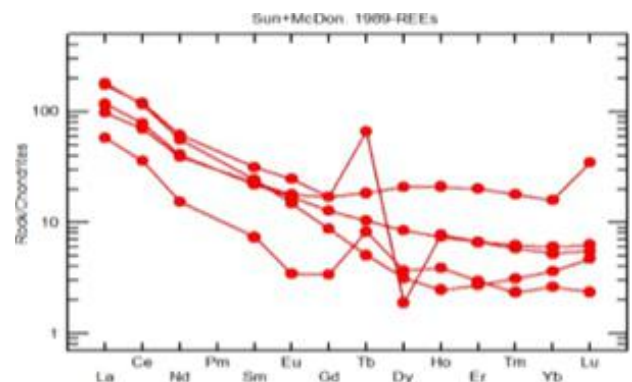


Fig. 17 - Chondrite-normalized pattern of REEs in all rocks of the region

#### 6 – Regional Tectonics

The regional tectonics results from activity of Qom – Zefreh faults in the northwestern part, end of Daruneh fault in the northwest of the region, Dehshir-Baft fault in the south, and end of ShahrBabak fault in the southeast, and also North Naein fault and Naein fault. In southern and eastern Shoja Abad, a shear zone is observed resulting from activity of strike-slip faults with north-south Qom-Zefrehstrike. The respective faulting zone have caused crushing of the rocks in the faulted zone and creation of suitable areas for rise of andesitic calc-alkaline magma



(with approximate Oligo-Miocene age) and alterations can be seen in the proximity of faults caused by hydrothermal solutions of the uplifting andesitic calc-alkaline magma. Furthermore, the most important feature of the respective section is presence of enclaves of oceanic crust type (with approximate Upper Cretaceous age) and uplift of the respective dark-colored masses during rise of calc-alkaline magma (Fig. 18). Also, boundary of enclaves is sharp with calc-alkaline magma matrix and lacks any alteration and demonstrates that andesitic calc-alkaline magmas have separated and elevated fragments from underneath during uplift but temperature of the rising magmas have not significantly affected the enclaves causing no alteration.

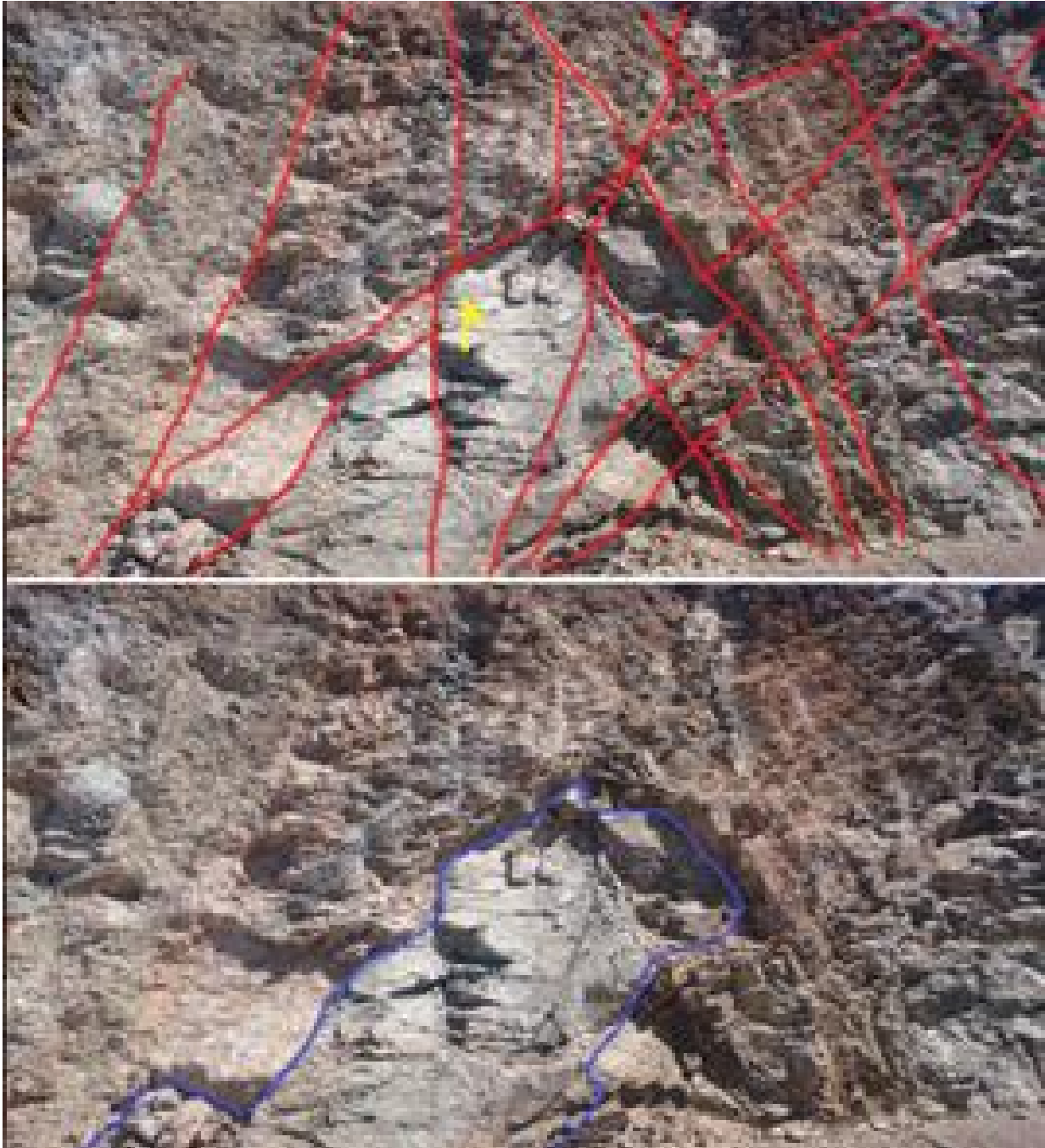


Fig. 18 – The uplifted enclaves of oceanic crust type along with andesitic calc-alkaline magams and strike-slip shear zone faults

The author believes that magmatism in the central part of the region under study and absence of regional metamorphism from the upper Precambrian onwards are indicative of absence of compression tectonic system in the studied region and can be attributed to the result of transformation of compressive energies into strike-slip movement of Qom-Zefreh fault in the relevant regions. Keeping in mind that the diagonal compression event in the subduction edge is provenance of the ophiolites of these regions influenced by exertion of compression in the generated compression ridges and creation of rift-like environment for occurrence of tholeiitic magmatism in the respective regions such that proximity of oceanic crust to the surface beneath the compression ridges causes emplacement of the constituent magma of the oceanic crust in the respective following spreading of the upper surfaces. Presence of sandstone as an indication of shallow marine environments adjacent to pillow lava representing deep ocean floor environments indicate floor spreading of a shallow sea floor in Lower Cretaceous and this extension continues into Late Cretaceous resulting in creation of oceanic crust in the respective regions. Following termination of tholeiitic basic magmatism and end of magma feeding by means of the detached oceanic crust and exertion of compression system in previous extensional ridges, calc-alkaline magmatism becomes predominant, and ultimately after detachment and rupture of the subducting plate, adakite and alkaninemasare are placed in the extensional fractures remaining from diagonal compression (Fig. 19).

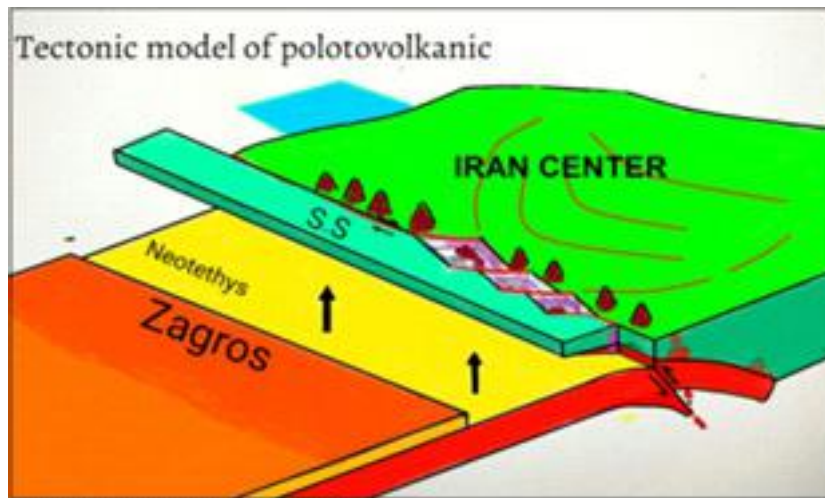


Fig. 19– Schematic model of diagonal compression of Neotethys subduction and creation of the affected extensional ridges

## 7– Conclusion

Eocene igneous series of Shoja Abad Region in northeast Esfahan have been invaded by Neogene and Plio-Pleistocene magmatism phase outcropping in the northwestern area of Shoja Abad Region and with composition of basalt, andesitic pyroxene, trachy andesite and trachydacite. The same magmatism has probably caused different alterations such as silicification, sericitization, and chloritization, and kaolinitization in the rocks of the studied area.

A magmatic series can be distinguished based on the chondrite-normalized diagrams of rare earth elements such that the diagram exhibits a declining trend for alkaline, calc-alkaline and shoshonite magmas and a flat or slightly ascending trend for tholeiitic magma series. Based on this evidence and according to other data, the samples belong to calc-alkaline magmatic series. High LREE/HREE ratio in the region is a sign of subduction zone.

Absence of magmatism in the central part and absence of regional metamorphism from Upper Precambrian onwards in the studied region reflect lack of compression system therein and it can be attributed to the result of conversion of compressive energies into strike-slip movement of Qom-Zefreh fault in these regions.

## 8– Acknowledgement

I am grateful to the researchers at the Azad university of North Tehran branch who have helped me in this study.

## References

- Agha Nabati S.A. (2006): Geology of Iran, Publications of Geological Survey and Mineral Exploration of Iran, 606.
- Alpers C.N. and Brimhall G.H. (1989): Paleohydrologic evolution and geochemical dynamics of cumulative supergene metal enrichment at la Escondida, Atacama Desert, northern Chile. *Econ. Geol.* 84, 229-255.
- Alpers C.N. Nordstrom D.K. and Ball J.W. (1989): Solubility of jarosite solid solutions precipitated from acid mine waters, Iron Mountain, California, U.S.A. *Sciences Géologiques, Bull.* 42, 281-298.
- Aja S. U. (1998): The sorption of the rare earth element, Nd, on to kaolinite at 25°C, *Clays and Clay minerals* 46, 103-109.
- Alderton D.H.M. Pearce A. and Potts P. (1980): Rare earth element mobility during granite Alteration: evidence from southeast England. *Earth Planet. Sci. Lett.*, 49, 149-165.
- Bau M. (1992): Rare earth element mobility during hydrothermal and metamorphic fluid-rock Interaction and the significance of the oxidation state of europium, *Chemical Geology*, 93, 219-230.
- Bissig T. Alan H. Clark and James K.W. Lee. (2002): Miocene Landscape Evolution and Geomorphologic Controls on Epithermal Processes in the El Indio-Pascua Au-Ag-Cu Belt, Chile and Argentina. *Economic Geology*. 97, 971-996.
- Desborough G.A. Kathleen S.S. Lowers, H.A. Swayze, G.A. Hannarstrorn. J. M. Deiehl, Sh F. Leinz R. W. Driscoll R.L. (2010): Mineral and chemical characteristic of some natural jarosite, *Geochemica et Cosinochimica Acta*, 74, 1041-1056.
- Dutrizac J. E. and Jambor J. L. (2000): Jarosites and their applications in hydrometallurgy. *Reviews in Mineralogy and Geochemistry* 40, 405-452.
- Dutrizac L.E. and Laniboi L. (2000): Jarosite and their application in hydrometallurgy. In *Sulfate Minerals, Crystallography, Geochemistry, and Environmental Significance* (eds. C.N Alpers, J.L. Jambor and D.K. Nordstrom). *Mineral. Soc. Am. Rev. Mineral. Geochem.* 40, 405-443.
- Fulignati P. and Sbrana A. (1998): Presence of native gold and tellurium in the active high-sulfidation hydrothermal system of the La Fossa volcano, Volcano, Italy. *J. Volcano Geotherm. Res.*, 86, 187-198.
- Haas J. R. Shock and E.L. Sassani D.C. (1995): Rare earth elements in hydrothermal systems: thermodynamic properties of aqueous complexes of the rare earth elements at high pressures and temperatures, *Geochim. Cosmochim. Acta*, 59, 4329-4350.
- Hedenquist J.W. and Browne P. R. L. (1989): The evolution of the Waitapu geothermal system, New Zealand, based on the chemical and isotopic composition of its fluids minerals and rocks, *Geochimica et Cosmochimica Acta*, 53, 2235-2257.
- Jambor J. L. (1994): Mineralogy of sulfide – rich tailing and their alteration products In the environmental geochemistry of sulfide mine – wastes (eds. J.L. Jambor and D.W. Blowes). *Mineralogical Association of Canada, Nepean*, 22, 59-102.
- Jambor J. L. (1999): Nomenclature of the alunite supergroup. *The Canadian Mineralogist* , 37, 1323-1341.
- Khodami M. (1998): Petrological Analysis of Volcanic Rocks of Northern Gavkhouni Swamp”, Master Thesis, University of Esfahan, page 170.
- Laufer F. Yariv S. and Steinberg M. (1984): The adsorption of quadrivalent cerium by kaolinite, *Clay Minerals*, 19, m-149.
- Lewis A.J. Palmer M.R. Sturchio N.C. Kemp A.J (1997): The rare earth element geochemistry-chloride geothermal systems from Yellowstone Wyoming, USA. *Geochim. Cosmochim. Acta*, 61, 695-706.
- Mehvari R. (2009): Petrological and Mineralogical Studies of Hydrothermal Alteration in Molla Ahmad Gorge, Master Thesis, University of Esfahan, page 310.
- Namnat A. (2011): Petrological and Mineralogical Study of Volcanic Rocks and Dependent Alteration Zones – KouhLokht Region-Toudashk (Southwest NAEIN), Master Thesis, University of Esfahan, page 110.
- Nordstrom D.K. (1977): Hydrogeochemical and

microbiological Factors Affecting the Heavy Metal Geochemistry of an Acid Mine Drainage System. Ph.D. thesis Stanford University, Stanford, California, USA.

- Parsapour (2004): Mineralogy of Hydrothermal Alteration in Rangan Region (Southwest Ardestan), Master Thesis, University of Esfahan, page 140.
- Rollinson H.R. (1993): Using Geochemical Data: Evaluation, Presentation, Interpretation, Lonman Scientific and Technical, 35p.
- Taghipour B. (2007): Mineralogy and Geochemistry of Thermal Alterations in Cenozoic Magmatic Arc of Central Iran (Esfahan Province) and Western Alborz, Taromsofla Zone (Qazvin Province), PhD Thesis, University of Esfahan, page 200.
- Taghipour B. and Mor F. (2008) : Geochemistry and Occurrence of Aluminum, Phosphate – Sulfate (APS) Group Minerals in Advanced Argillic Alteration Zone of Northwest Shirkouh, Yazd, Journal of Economic Geology, 153 – 165.
- Scott K. M. (2000): Nomenclature of the alunite supergroup: The Canadian Mineralogist, 38, 1295-1297.
- Stoffregen R.E., Alpers C.N., and Jambor J.L. (2000) Alunite-jarosite crystallography, thermodynamics and geochronology. Reviews in Mineralogy and Geochemistry 40, 453–479.
- Swayze G.A. Desborough G.A. Smith K.S. Clark R.N. Sutley S.J., Pearson R.N. Rust G.S. Vance L.S. Hqgeinan P.L. Briggs P.H. Meier AL. Singleton and Roth S. (2000): Using imaging spectroscopy to map acidic mine Waste, Environ, Sci. Technol, 34, 47-54.
- Wenlandt R.F. and Harison W.G. (1997): Rare earth partitioning between immiscible carbonate and Rare Earth enriched rocks, Corti 6. Mineral petrology 69, 409-419.
- Wise W.S. (2000): Solid solution between alunite, woothuosite and canadallite mineral series .N. Jb\_ Mineral, Mn. 540-545.
- Wood S. A (1990): The geochemistry of rare earth elements and yttrium, theoretical prediction of speciation in hydrothermal solution to 350 °C at saturation water vapour pressure, Chemical Geology, 88, 99-125.
- Zanetti A. Mazzucchelli M. Rivelenti, G. & Vannunci